In-line metrology of nanoscale features in semiconductor manufacturing systems

Tsung-Fu Yao, Andrew Duenner, Michael Cullinan*

Department of Mechanical Engineering, University of Texas at Austin, United States

ARTICLE INFO

ABSTRACT

Quality control and defect monitoring are of great importance to the semiconductor industry. This article presents a system to enable inspection of nanoscale features in-line with nanomanufacturing processes. The ultimate goal of this research is to integrate this metrology system into current semiconductor manufacturing processes to enable true in-line wafer inspection and quality control. In the system presented in this paper, AFMs that have been shrunk down on to a single MEMS chip are used to scan the surface of a sample. A flexure-based mechanism allows the MEMS-based AFM to be positioned over a millimeter range of motion, with nanometer level precision when properly actuated. The performance of the system in areas such as positioning repeatability, AFM stability and measurement resolution are evaluated in this study. Owing to the small size of single-chip AFM (1 million times smaller than a conventional AFM instrument), it is a good candidate for multipoint detection. Overall, the system presented in this paper significantly shortens inspection time and dramatically decreases the setup time required for an AFM to load, approach, and measure a sample making in-line inspection of nanoscale features in semiconductor manufacturing systems feasible.

1. Introduction

Nanoscale manufacturing techniques enable technologies used in many aspects of daily life. The most common use of nanoscale manufacturing is in the production of integrated circuits (ICs) and microchips, which consist of billions of transistors and other electronic components in a small area (in mm² scale). These transistors are typically patterned in batches on silicon wafers and the critical dimension (CD) of these transistors has fallen from the micron scale to tens of nanometer over the last 25 years. In addition to the semiconductor manufacturing industry where many nanofabrication technologies were initially developed for the mass production of integrated circuits, many new nanomanufacturing processes are emerging for the photonics, energy, and healthcare industries where more complex three-dimensional structures are required [1–3]. As features continue to decrease in size and increase in complexity quality control and yield analysis become increasingly difficult. Therefore, metrology for nanopatterning is an important issue for detecting errors and reducing waste before the patterned wafer moves on to the next processing step.

Measurement of manufacturing processes can be performed either in-line as part of the manufacturing process or off-line in a separate process. Unfortunately, no methods currently exist to measurement nanoscale features in-line with high-rate nanomanufacturing processes. Therefore, inspection, if it is done at all, generally takes place offline using slow metrology methods such as atomic force microscopy (AFM) or scanning electron microscopy (SEM). However, in-line semiconductor inspection has several real advantages compared to off-line inspection. First, in-line inspection eliminates steps such as sample loading and unloading from the main assembly line for inspection. This results in an increase in throughput of chips that can be handled per unit time. In-line wafer metrology also decreases the time required to observe problems in the manufacturing process. As such, defects in masks and dies can be detected sooner and remedied earlier to increase yield. Finally, in-line inspection can be used to implement statistical process controls in order detect equipment issues before they lead to defects in the final manufactured product.

The limiting factors to enabling in-line nanoscale metrology are the resolution of the metrology tools and the total time required to take a measurement sample using present technologies. Decreasing the total time required to prepare and measure a sample is the key to enabling in-line inspection in nanofabrication. While a number of technologies are capable of imaging nanoscale features, advances

* Corresponding author.
  E-mail address: michael.cullinan@austin.utexas.edu (M. Cullinan).

in atomic force microscopes (AFMs) show promise for enabling true in-line metrology. High-speed AFM imaging techniques have been in development for many years. Currently, two methods exist for increasing AFM scanning throughput [4]. One method is to utilize an array of cantilever scanning tips instead of the traditional single tip. A second method for increasing throughput is to increase the scanning speed of a single tip. This method requires an increased resonant frequency because most of the commercial AFM instruments are already operating at frequencies close to their resonant frequencies. One way to increase the resonant frequency of the sensing cantilever is to reduce the dimensions of the AFM system. Conventional AFMs have a large number of components and have large moving masses but if the system is scaled down into a single MEMS chip it becomes possible improve the scan speed of the AFMs. This miniaturization also allows multiple, independent AFMs to be assembled into the production line enabling metrology to be directly embedded into nanomanufacturing system.

In this paper, we propose a new method for semiconductor metrology which incorporates multiple single-tip AFMs attached to a stage which can be rapidly brought into contact with the wafer to be measured [5]. In a typical inspection system, it is desirable to measure the same points on the wafers for each inspection. Therefore, the positioning repeatability of the AFM cantilever relative to the sample in an AFM system needs to be better than the scanning range of the AFM system, which is typically on the order of a few microns. In order to achieve this level of repeatability, a kinematic coupling is used to repeatably position the AFM stage relative to the wafer mounting stage. The AFM inspection system itself utilizes MEMS-based components such as flexures, actuators, and sensors to drive a microscale cantilever for high speed measurements [6]. This method allows for the rapid measurement of nanoscale features over the surface of a wafer. In the system presented in this paper, each single-chip AFM is mounted on a 2D stage that allows course-positioning translation over a 1 mm range and nanometer repeatability when the stage is lifted to accommodate a wafer sample. The presented system uses flexure bearings because of both the mechanical simplicity and high precision of flexures [7]. Moreover, because of the compact nature of the flexural bearing system, the inspection system presented in this paper has the potential to simultaneously utilize multiple MEMS-based AFMs within the confined area of the wafer surface in order to increase the area that is measured within a single metrology step. However, this paper focuses on the operation of a single AFM chip within the inspection system and presents the performance of the single-chip AFM inspection system including the error motion of X-Y flexure system, the repeatability of translation in each axis, and the stability of the single-chip AFM operation. Moreover, this paper investigates the cycle time and imaging resolutions of measurement with the system and proves the feasibility of the system for in-line inspection of nanoscale features.

2. Background

Geometric dimensions such as line edge roughness and sidewall angle are measured to ensure that tolerances are being maintained in nanomanufacturing processes. There is an extremely low margin for defect error in the manufacture of components such as processor dies. Producing components such as patterned media for memory requires excellent uniformity and tolerances for individual defects are somewhat relaxed [8]. The ideal nanomanufacturing metrology system would be capable of rapidly characterizing nanometer scale local defects and feature uniformity over a patterned area of a few hundred centimeters squared. Present technologies are limited to either high throughput metrology of average features or extremely low throughput metrology of individual features. Table 1 provides

a comparison of existing metrology technologies and Fig. 1 illustrates resolution and throughput within metrology technologies. Note that the scanning areas are not standardized but the throughput must be based on not only the ratio of area and scanning speed, but also the sample preparation and uploading/unloading operation. Table 1 and Fig. 1 are just showing an approximation in scan time, the actual scan time is highly depending on the whole sample area in measurement. However, Table 1 tells that the bottleneck of throughput is the setup time, which takes up most of the measuring cycle time in each metrology technology.

Optical scatterometry is a metrology technology that can be utilized to measure average feature geometry with sub-nanometer resolution [12]. Optical scatterometry equipment detects changes in reflected light and through computational analysis of the reflected light yields information on average geometry [15]. Advanced metrology systems based on optical scatterometry are used in industry to detect overlay errors and add only 15 s of overhead per wafer [16]. Optical scatterometry is capable of high-throughput metrology with nanometer resolution, but its use is limited to determining average dimensions of dense repeated patterns.

Instruments such as the scanning electron microscope (SEM), scanning tunneling electron microscope (STEM) and atomic force microscope (AFM) are routinely used to characterize individual features at the nanometer scale. It is possible to resolve features down to the angstrom level with STEM and AFM and to the single nanometer level with SEM [9]. Presently all of the systems that are capable of resolving individual nanoscale features are used offline and are not suitable for in-line metrology in nanomanufacturing systems. Electron microscopes generally require vacuum [17] and use high energy electron beams that can damage sensitive substrates [9]. Furthermore, electron microscopy is only suitable for conducting samples.

Atomic force microscopy shows promise as a technique to enable high throughput nanometer scale in-line metrology. As compared to other metrology technologies such as optical scatterometry and SEM, the limitations of AFM are not inherent to its operating principle. The challenges of range and scanning speed can be solved while maintaining the basic operating mode and high resolution of a traditional AFM system. AFM metrology typically uses a single oscillating cantilever beam to laterally scan the surface of a sample. Current AFM systems are not suitable for in-line metrology due to limited lateral range and relatively slow scanning speed. The scan speed of AFMs are typically on the order tens of microns per second [4] due to attenuation of resonant stage frequencies at higher speeds. As the scan speed approaches the resonant fre-
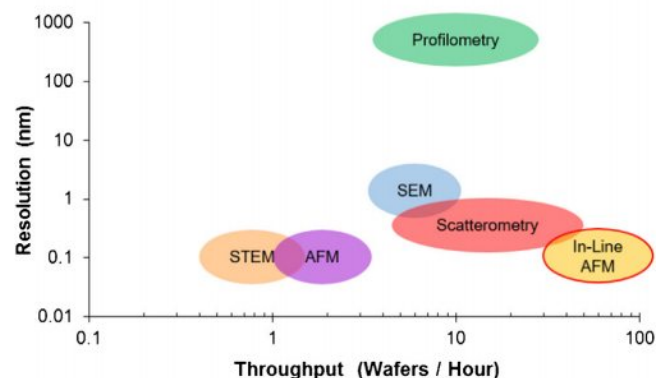

Fig. 1. CD Metrology Resolution vs. Throughput.

Table 1
Performance Comparison of Nanomanufacturing Metrology Technologies.

Technology	Vertical Resolution	Setup Time	Scan Time/Wafer	Sites/Wafer	Limitations
SEM	1.35 nm [9]	20 min	1.5 min [9]	5 [9]	Vacuum, sample damage [9]
Automated STEM	<0.1 nm [9]	75 min [10]	10 min [11]	1	Sample Damage
AFM	<0.1 nm	20–30 min	1–2 min [9]	1	Slow speed
Contact Profilometry	0.1 nm	20 min	5 min	1	Poor Lateral Resolution [12]
Optical Profilometry	<0.1 nm	20 min	12 min [13]	1	360 nm Lateral Resolution [13]
Optical Scatterometry	0.4 nm [9]	4 min [14]	10 s [14]	1	Insensitive to variations within spot size [9]

quency of the measurement stage, probe drift can be induced by the vibrations of the stage [18]. Vibration induced error motions cause the image to be distorted, and usually this source of error is negligible at lower operating frequencies. As a result, commercial AFM instruments usually require several minutes to finish a measurement over an area of several square micrometers. Current AFM systems are limited to a small scanning area due to the challenge of designing a stage to move with nanometer resolution. Piezoelectric and thermal actuators are commonly utilized components for moving the cantilevered AFM tip relative to the sample. These actuators, chosen for exceptional positioning resolution, are inherently limited to displacements on the order of microns.

Increasing the stiffness of an AFM scanning stage allows for higher operating speeds. One straightforward method for increasing the stiffness of a system is to decrease its size. Because mass is proportional to the cube of length and stiffness is linearly proportional to length, resonant frequency of a system is inversely proportional to its characteristic length ($\omega_n = \sqrt{k/m}$). Resonant frequencies as high as 1.3 MHz have been achieved by decreasing the length of the oscillating cantilever on an AFM system [19]. In a later study, Hansma et al. [7] designed and tested a scanning stage that minimized the length of the cantilever as well as the mechanical working length of the flexural elements utilized to decouple motion of the stage axes. Hansma's cantilever system was capable of scanning at a rate of 7810 lines per second and demonstrated video rate imaging with a resolution better than 200 nm.

MEMS-based structures allow for extremely high resonant frequencies because the microscale features typically have high stiffness to mass ratios. The first MEMS-based AFM instrument was designed and fabricated by Hierlemann et al. [20]. The device consisted of an array of cantilevers on a single chip. Each cantilever was essentially an independent AFM capable of individual actuation, sensing, control and processing. Disseldorp et al. [21] developed a high-speed MEMS-based AFM with out-of-plane scanning motion. The high-speed z-scanners were capable of achieving a maximum tip speed of 5 mm/s without inducing resonance. Recently, Sarkar et al. [6,22,23] announced a single-chip AFM which integrated all of the electrical and mechanical components onto a single chip made by CMOS-MEMS process. Sarkar's single-chip AFM is capable of imaging over a range of 25 μm with nanometer resolution in the Z-direction. The single-chip AFM has imaging resolution and range which is competitive with current commercial instruments with the further advantage of extremely small size and low cost. The single-chip AFM is to date the best imaging solution for integration into a system for in-line metrology in semiconductor manufacturing.

Another method to increase AFM metrology throughput is to utilize an array of cantilevers instead of a single cantilever. Increasing the number of cantilevers results in an increase in the amount of data scanned at one time. Several studies [20,24,25] have demonstrated the use of cantilever arrays to increase AFM imaging throughput. Even though the cantilever array does not actually speed up the imaging operation, the use of multiple cantilevers makes it possible to gather the information over an extended area thus increasing the throughput of the system. Existing AFM
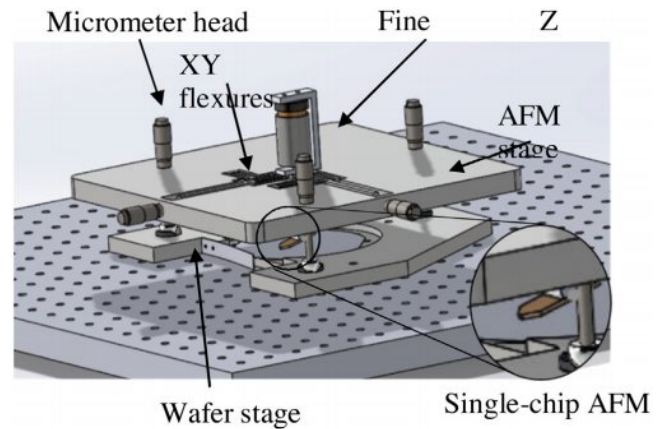

Fig. 2. Overall schematic of inspection system with single-chip AFM.

cantilever array designs do not allow independent X-Y-Z actuation of the individual cantilevers and are limited to scanning over relatively limited ranges. However, MEMS based cantilever array systems could be the key to overcoming these limitations.

3. Description of system

The system presented in this paper utilizes a single-chip AFM affixed to a flexure stage to enable in-line metrology of semiconductor wafers. The in-line inspection system consists of two stages. The first stage consists of flexure for positioning the AFM chips in the X and Y directions and a second flexure mechanism for positioning the chip in the Z direction. The XY flexure mechanisms on the AFM stage allow the AFM chip to be precisely positioned relative to the feature being measured on the silicon wafer. Out-of-plane motion is minimized due to the decoupled flexure design. The stage provides approximately 2.6 mm of translational range in the X and Y directions. A second flexural element is used to allow motion in the Z-Direction. The flexure utilizes a double parallelogram design with compliance in the Z-direction and high stiffness in other directions. The Z-flexure is coupled to a voice coil linear actuator (LVCM-025-038-01, MotiCont) with motion resolution better than 10 nm. This Z flexure system allows for a positioning range of approximately 0.5 mm.

The second stage is a passive wafer alignment stage, as shown in Fig. 2, which is used to position the wafer with a repeatability better than 1 μm [26]. The two stages are mated using three kinematic couplings. The kinematic couplings on the wafer alignment stage interface with half-balls attached to micrometer heads on the AFM stage. The micrometers can be used to coarsely adjust the pitch, roll, and height of the AFM chip. The kinematic coupling mechanism ensures the relative position between both stages is highly repeatable after loading and unloading operations.

In this in-line metrology system, the silicon wafer is first placed into the passive alignment mechanism of the wafer stage. The AFM stage is then placed on top of the passive wafer alignment mechanism and aligned to the wafer using a kinematic coupling. The

XY flexure stage is only used the first time a wafer is loaded into the system. After the AFM chips are positioned relative to points of interest on the silicon wafer, the passive alignment mechanism and kinematic couplings are sufficient to ensure that the same spot is measured on each subsequent wafer that is loaded into the system. Once the wafer is loaded into the system and the AFM stage is placed onto the kinematic couplings, an actuator applies a force to the Z-Axis flexure and the AFM chip is translated to a distance from the wafer that is within the sensing range of the AFM chip. After the measurement is taken, the AFM retracts and the AFM stage and wafer can be removed to allow another wafer to be placed into the system. These rapid alignment systems allow the time between measurements to be reduced to less than one minute. Fig. 3 shows the process flow of the inspection system.

In this study the single-chip AFM [6] is able to image a sample with nanoscale features in over an area of 30 μm × 12 μm. As shown in Fig. 4, the chip contains all of the components of an AFM including the scanner, actuator, and resonator. A signal amplification circuit and electronics for operating the single-chip AFM are contained in a box separate from the AFM chip. The AFM chip is mounted to the z-approach stage at about 15° related to the wafer that is being inspected.

3.1. Single-chip AFM

This in-line inspection system utilizes the single-chip AFM (Single-Chip Atomic Force Microscope, ICSPI Corp.) The single-chip AFM includes all of the electromechanical components of an AFM in a small chip. The layout of electromechanical components for the single-chip AFM is shown in Fig. 4. The chip consists of a scanning assembly including electrothermal lateral actuators and a vertical bimorph for moving the cantilever tip relative to the surface of the sample. The chip also contains strain gauges to measure the interaction force between the tip and sample. This device is operated in a constant-amplitude mode that maintains a constant oscillation amplitude of the cantilever when scanning. When the cantilever tip approaches the surface of the sample, the amplitude is weakened due to the interaction forces between the tip and the sample. Closed-loop feedback is utilized to maintain a constant height of the cantilever relative to the surface sample. When the tip is closer to the wafer, oscillation amplitude decreases and the AFM chip inputs a higher voltage to the Z-actuator. The magnitude of the voltage output to the actuator is recorded, and with calibration can be used to extract topography information. The lateral scanning in the AFM
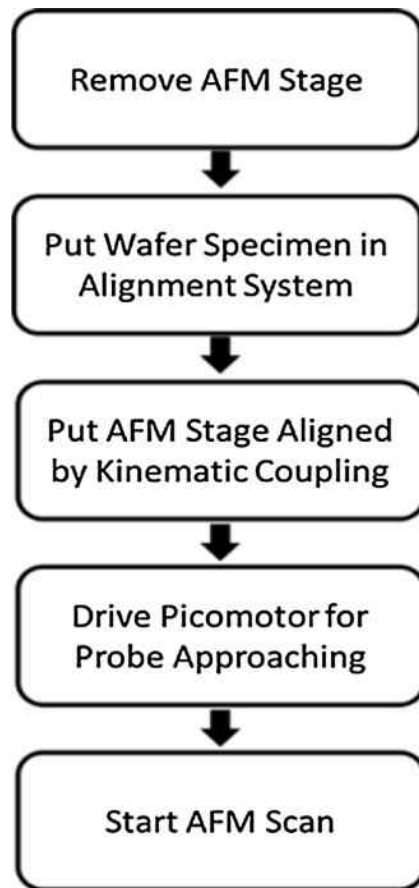

Fig. 3. Measurement Procedure in the in-line inspection system.

chip is accomplished via extension and contraction of electrothermal flexural actuators, which allow for one translational DOF and one rotational DOF.

3.2. Design of XY linear stage

The XY parallelogram flexure stage was designed utilizing a constraint map [27]. Fig. 5 shows the flexure bearing layout. Flexure elements *a.* and *b.* are compliant in the X-direction and flexure elements *c.* and *d.* are compliant in the Y-direction. The actuation force
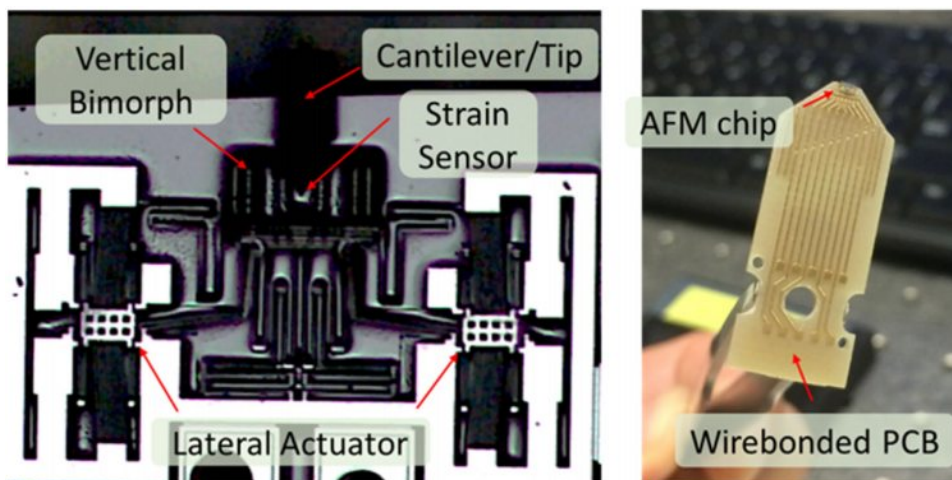

Fig. 4. (Left) Microscope image of the layout of single-chip MEMS-based AFM and (Right) photograph of PCB daughter board that is used to breakout the leads from the AFM chip.
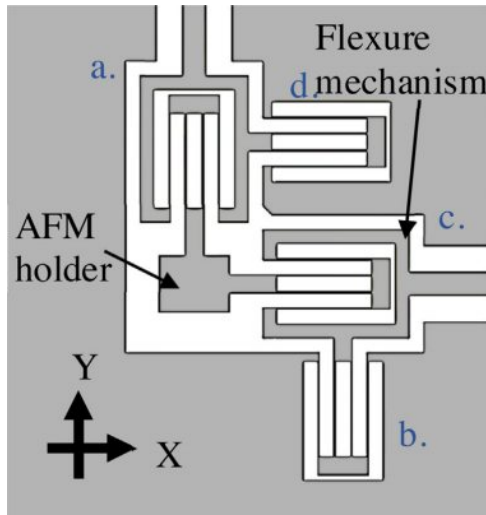
Fig. 5. AFM stage with flexure-based positioning (Top-view).

Fig. 6. stress simulation for positioning flexure (50 N exerting force with aiuminum 7075-T651 material).

is applied to flexure elements *a.* and *c.* while elements *b.* and *d.* are connected to ground. Previous studies [27] have shown that the tangential stiffness of a double parallelogram flexure is a function of beam element geometry. The stiffness could be written as:

$$K_t \sim \left[12 - \frac{3}{100} \left(\frac{F_a L^2}{EI} \right)^2 \right] \cdot \frac{EI}{L^3}$$

where L is flexure beam length, E is Young's modulus, I is the second moment of area for the flexure beam and F_a is external axial force. The effective stiffness of the positioning flexure layout is equal to twice of a tangential stiffness due to the parallel configuration. A 5/8″ thick sheet of 7075-T651 aluminum was chosen as the flexural material due to its high yield strength to elastic modulus ratio. The axial force is provided by micrometer heads with a maximum force of approximately 50 N. The stiffness of the system was chosen such that displacement of greater than two millimeters is obtainable with a force of less than 50 N. A beam thickness of 0.4 mm was chosen for the flexures due to the minimum machinable thickness on the waterjet cutter. With constraints on elastic modulus, beam thickness, width, and axial force, it was determined that a 20 mm flexure beam length yields overall stiffness of 19.4 N/mm (shown in static simulation), which gives a 2.58 mm displacement with 50 N of exerted force. The stress state while operating in maximum displacement is examined by finite element method. The simulation (Fig. 6) shows that the maximum stress in the flexure at its maximum displacement is approximately 3.29×10^8 N/m² which is well below the yield strength of 7075-T651 aluminum (5.05×10^8 N/m²). The parallelism errors of stage motion that result due to manufacturing errors were determined by measurement of the fabricated stage.

3.3. Design of Z axis flexure

Accurate Z positioning is essential for an AFM to operate correctly. AFM cantilevers must approach to the sample before scanning, and resolution in the Z-direction must be on the order of 40 nm to avoid crashing the tip into the sample. This system utilizes a voice coil driven by a precision linear amplifier circuit that provides positioning resolution of better than 10 nm over a range of several millimeters. The actuator is capable of 11 N of axial force. Two double parallelogram flexures in parallel are utilized to couple the actuator to the AFM chip and to constrain motion to translation in the Z-direction. An illustration of the flexure is shown in Fig. 7a.
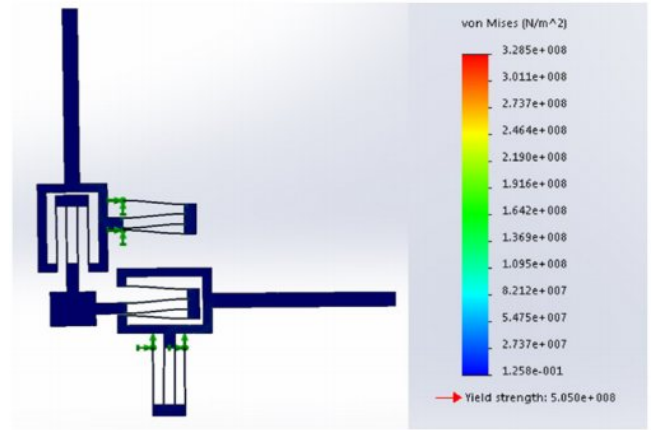
The symmetric double-parallelogram design was chosen to maximize the linearity of motion. 7075-T6 Aluminum was chosen as the flexure material due to its high ratio of yield strength to elastic modulus ratio. The beam width was limited to the 10 mm width of the flexure stage and the beam thickness was limited to the 0.4 mm minimum thickness limitation of the waterjet used to machine the flexure. The length of the flexure beams was chosen so that 11 N of axial force would allow for a displacement of 0.5 mm. FEA analysis was utilized to simulate stresses in the flexural bearing. A force of 11 N yielded a maximum displacement of 0.568 mm and a maximum stress of 65.6 MPa which corresponds to a safety factor of 7.67. The results of the FEA analysis are shown in Fig. 7b.

3.4. Z-Approach procedure

The inspection system moves the AFM chip into close proximity with the surface of the wafer in three stages before scanning. After a silicon wafer is placed into the passive wafer alignment stage, micrometer heads are utilized as a coarse approach mechanism to move the chip stage relative to the wafer alignment stage. This step is only needed the first time a wafer is loaded into the system since the kinematic couplings are repeatable enough that course adjustments can be eliminated for all subsequent loading operations. Once the chip is at a distance of approximately 0.5 mm from the wafer surface, the voice coil actuator is utilized to provide precise positioning. Feedback of tip-sample distance is introduced from the oscillation amplitude signal of the AFM chip. A precision voice coil drive circuit was constructed to convert the voltage signal from the feedback loop to current output to the voice coil. The circuit for the voice coil driver is shown in Figure and its block diagram is shown in Fig. 8. Fig. 10 shows a scheme that explains the fine approach control by voice coil actuator cooperating with the AFM sensor. The control loop set point is chosen to be one-half of the amplitude signal of the cantilever when the cantilever is oscillating in free space. When this set point is reached, the voice coil current is locked and the AFM scan starts. A thermal bimorph on the AFM controls tip sample distance with nanometer precision during the scan.

3.5. Kinematic coupling design

Kinematic couplings are capable of highly repeatable positioning and are often used when two components must be precisely positioned relative to each other but still remain separable. Kinematic couplings also have the advantages of self-alignment, low cost, and simplicity. A proper kinematic coupling has an equal num-
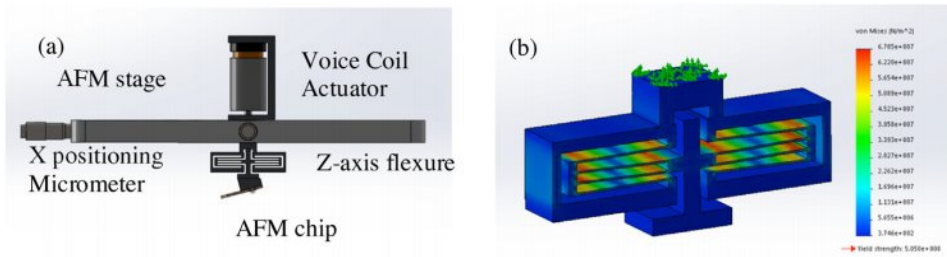
Fig. 7. (a) Working concept of the Z-axis flexure in in-line inspection system (b) Z-axis flexure FEA stress analysis.
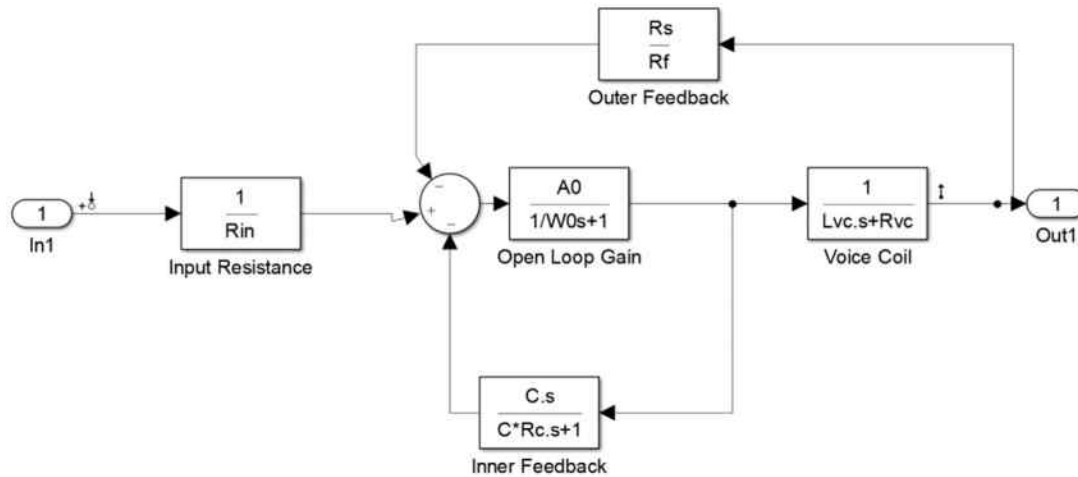

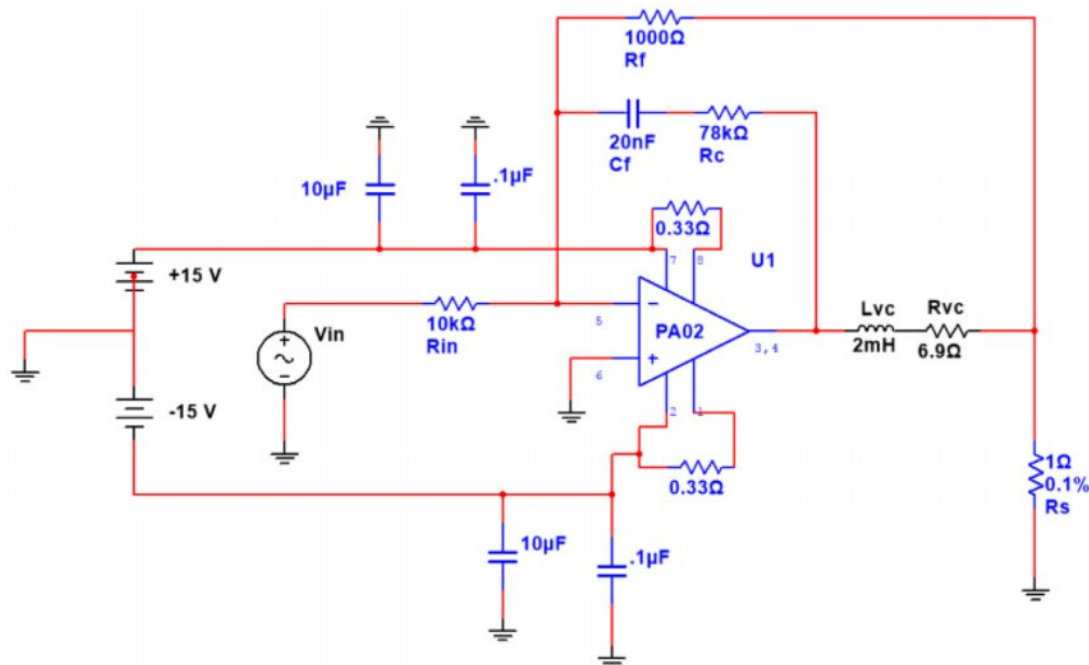**Fig. 8.** Voice Coil Drive Circuit Block Diagram.

Fig. 9. Voice Coil Drive Circuit Diagram.

ber of contact points and constrained degree of freedom [28]. All six degrees of freedom are constrained between the chip stage and the wafer alignment stage. Each kinematic coupling contains a hemisphere (to provide a ball surface minimizing the contact point) and a v-groove, as shown in Fig. 11. The contact between the ball and

the v-groove constrains two degrees of freedom. Fig. 12 shows the layout of the three couplings in the wafer stage, each coupling is located at apex of an equilateral triangle. The hemispheres are bonded to a micrometer head, which is fixed to the AFM stage. The micrometers can be adjusted together to change the distance
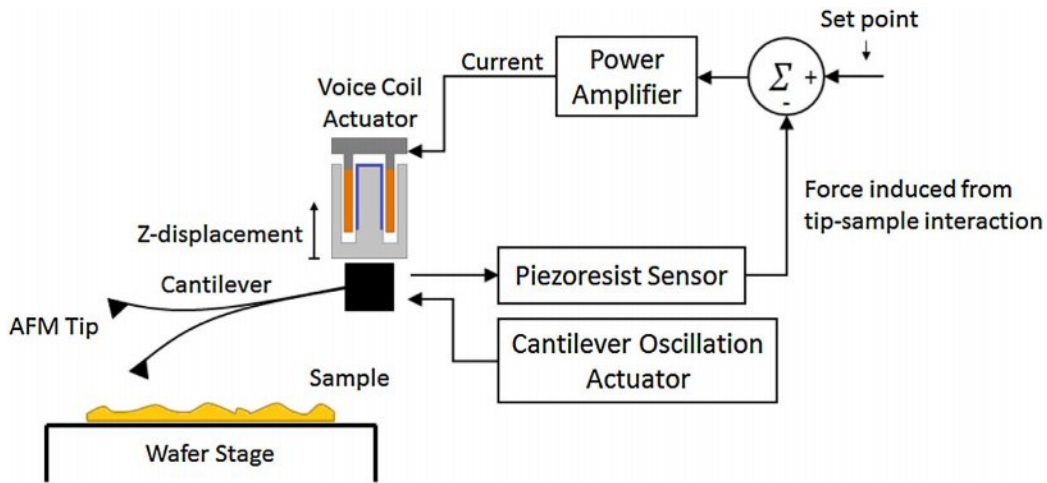
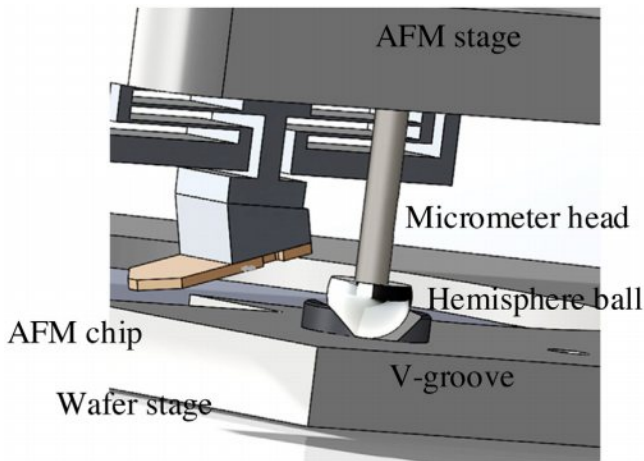**Fig. 10.** Fine z control with AFM signal sensor and VCM actuator.

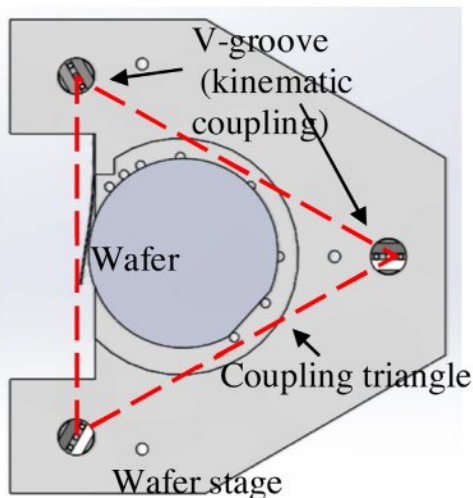**Fig. 11.** Schematic of kinematic coupling between AFM stage and wafer stage.

Fig. 12. Kinematic coupling layout on wafer stage.

between the chip stage and the wafer stage or independently to change the pitch and roll of the chip stage relative to the wafer stage. Overall, this system allows for highly repeatable alignment of the AFM chips relative to the wafer between wafer loading steps.

4. System fabrication

The XY flexural stage was waterjet cut from a single block of 7075-T651 aluminum. This material was chosen due to its high strength to stiffness ratio and its relatively low thermal expansion coefficient. Waterjet fabrication limits the thickness of all flexural elements to a minimum thickness of 0.40 mm. Due to the chamfer inherent in waterjet cutting of thick plates (5/8th of an inch in this case), the 0.40 mm thick flexural elements on the XY stage ended up having a non-rectangular profile with a thickness of 0.30 mm at the top and 0.60 mm at the bottom. While the variation in flexural element thickness did cause some variation between modeled and actual stiffness, the flexures maintained their characteristic repeatability.

After the waterjetting process, a number of holes were CNC drilled into the stage to accommodate the coarse approach micrometers. Holes for the micrometers were sized for a close clearance fit and nuts were utilized to fix the micrometers to the stage. Couplings were machined to allow the non-threaded micrometer shafts to attach to precision half balls. The micrometer shafts and the precision half balls were bonded to the couplers using a Loctite retaining compound.

The Z flexure was also waterjet cut from a block of 7075-T651 Aluminum. The thickness of the flexure elements was chosen to match the 0.40 mm minimum thickness attainable on the waterjet machine. The flexures were carefully sanded by hand in order to reduce variations in thickness which might cause the overall stiffness to be too high for the limited force of the voice coil linear actuator. Before mounting the Z flexure to the XY stage, a threaded hole was drilled and taped for the actuator. The Z flexure was bonded to the stage using Loctite 430 cyanoacrylic glue formulated for use on aluminum. Finally, an angled adapter was machined to accommodate the AFM chip and to maintain an angle of approximately 15° between the sample and the chip. The chip was positioned on the adapter with two 1 mm dowel pins and held in place by a low profile screw. The fabricated XY stage and Z approach mechanism are shown in Figs. 13 and 14.

5. Results

5.1. Parallelism in XY flexure positioning

Parasitic error motions in the flexure stage are caused by imperfections in the fabrication of the flexures. In addition, the actual X and Y axes are not perfectly decoupled and deviation between
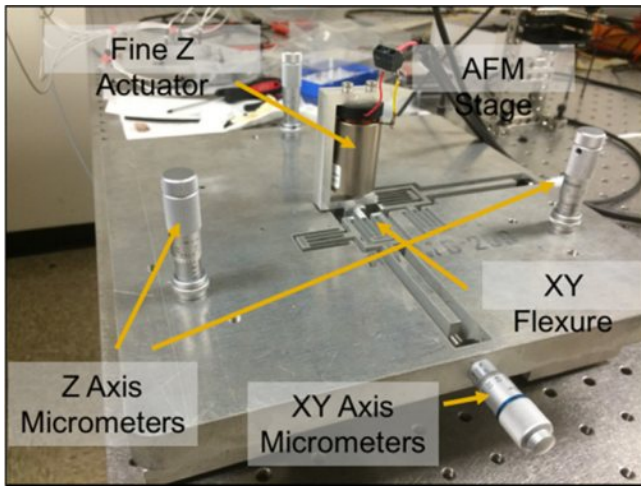
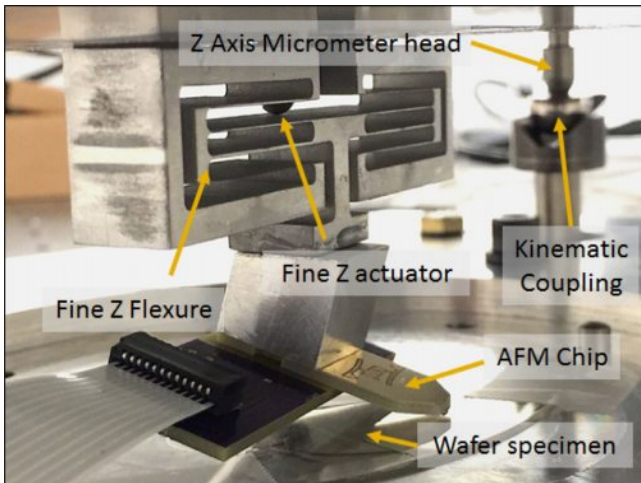**Fig. 13.** Fabricated in-line dimensional metrology system setup.

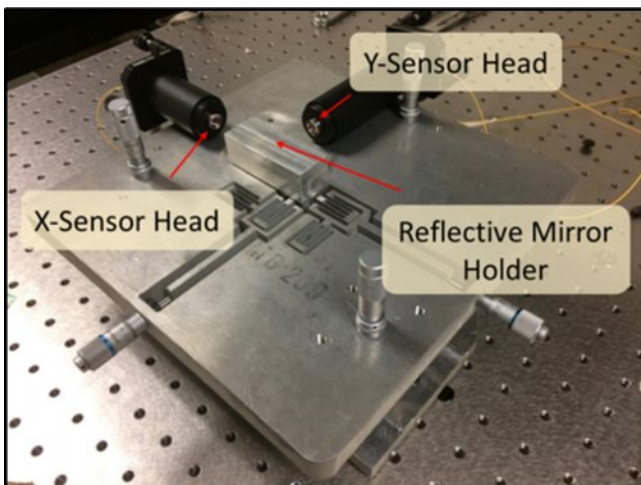**Fig. 14.** Fabricated Z flexure mechanism.

Fig. 15. Experiment setup of the parallelism test for XY positioning.

true and ideal motion may cause problems when operating the stage. Therefore, a measurement for parallelism is necessary before putting the system into practice. Fig. 1 shows the parallelism test setup for the XY flexure positioning stage. A fiber-based, inter-ferometric measurement system (FPS3010, Attocube) with 1 pm
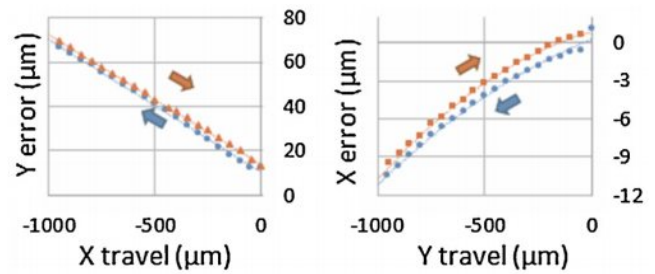

Fig. 16. Parasitic error motion in Y and X directions while X and Y is traveling within 1.0 mm.

displacement resolution [29] was used to measure for the para-sitic error motion while one axis was actuated with a micrometer. The measurement system used two sensor heads (Sensor Head M12/C1.6, Attocube; 1000 mm linear measurement range) con-nected via fibers to transmit and receive laser beams used to measure displacement.

The wafer stage and two sensor heads were mechanically grounded to an optical table. One carefully polished rectangu-lar block was mounted to the AFM chip stage. Two mirrors were attached to the block with surfaces normal to the X and Y directions. The mirrors reflected the laser beams transmitted from the sensor heads. The error motions were measured by actuating a microm-eter a distance of 1.0 mm in X or Y direction and recording the parasitic displacement in the direction orthogonal to the actuation axis. Fig. 16 shows the recorded parasitic error motion in Y and X directions. The parallelism test shows the parasitic Y motion is lin-early related to translation in the X axis with a slope of 59.9 μm per 1.0 mm motion. On the other hand, the parasitic X motion behaves with a quadratic relation to Y motion, with 11.1 μm of parasitic motion in the first 1.0 mm motion. Based on these results, the par-asitic error in both directions will be about 100 μm over the entire 2.58 mm operating range. This the parasitic motion is compensated for over the full range of the stage by making fine adjustments to the actuators in the off axis direction of motion based on the measured parasitic errors.

5.2. Repeatability in positioning system

This in-line inspection system is designed to repeatably examine the same location on wafer samples. The system will require that samples are repeatedly loaded and unloaded without affecting the position scanned on each sample. A typical atomic force microscope provides a scanning range of a few micrometers. As such, tradi-tional positioning stages for an AFM require nanoscale positioning repeatability. The stage presented in this paper requires overall wafer positioning repeatability better than the 15 μm scanning range of the single chip AFM. A passive wafer alignment mecha-nism is utilized to seat the wafer against three pins. Wafers inserted into this system self-align and repeatability on the order of 1 μm has been demonstrated [26]. One potential source of error in the design is the repeatability of the kinematic couplings that align the wafer stage with the AFM stage.

In order to determine the magnitude of this error source, four capacitance probes (CPL 290, LION Precision), with 0.14 nm resolu-tion and 2.0 mm working range [30], were fixed to the optical table as shown in Fig. 17. One probe was used to determine displace-ment in the X direction and two probes perpendicular to the first were used to determine displacement in the Y direction and rota-tion about the z-axis. The fourth probe was mounted on the AFM stage and measured displacement in the Z-direction relative to the wafer stage.
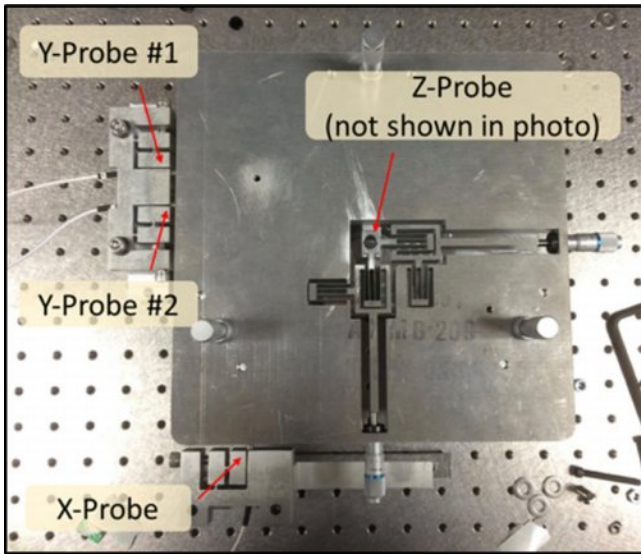
Fig. 17. Experiment setup of the repeatability test for specimen replacement in positioning system.

The repeatability results are shown in Fig. 18. The test was performed by attaching and detaching the AFM chip stage to the wafer stage and measuring the difference between the original stage position and the position of the stage after the reattaching operation. The test was performed 48 times and the repeatability was calculated as the sample standard deviation of the trials. Because the number of trials is large, the sampling standard deviation is expected to be a good representation of the population standard deviation. The results indicate repeatability of about 390 nm, 361 nm, and 60.0 nm in the X, Y and Z directions respectively. Rotational repeatability about the Z-axis was 140 nrad.

5.3. Stability measurements

The single-chip AFM presented in this paper operates in amplitude-modulated AFM mode. In this mode of operation, the cantilever maintains constant oscillation amplitude while scanning the sample surface. Tip-sample interaction forces create an error signal between commanded and actual oscillation amplitude. The controller increases or decreases the voltage sent to the Z-actuator and the amplitude of the correction signal is recorded as a function of the X and Y position of the cantilever. The recorded signal is proportional to the distance between the tip and the sample and is used to determine the topography of the sample. A number of noise sources exist in the system that can affect the signal from the AFM. The signal used to drive the voice coil actuator may introduce electrical noise and mechanical vibration between components is another source of noise. Noise was observed when the z-approach mechanism was being actuated. The estimated RMS signal-to-noise ratio was observed to be approximately 28.8 dB.

The AFM chip controller adjusts the modulating signal to account for the effect of drift; however, when the drift amount is beyond the maximum voltage that modulation could provide, the scan will fail. The single-chip AFM used in the inspection system has a maximum modulating signal of 3.0 V. The direction of the observed drift was variable with respect to the sample depending on the initial conditions on the stage but was not found to be sample dependent. In order to determine the extent of the drift, the amplitude of the AFM signal was measured over a 7-h time period. Ambient temperature was also measured during this time. Fig. 19 shows the AFM signal and ambient temperature over time. It was predicted that fluctuations in temperature would influence the drift of the AFM tip significantly. The data collected, however, does not show any correlation between temperature and AFM signal. As such, the drift must be attributable to other phenomena such as vibration, electromagnetic interference, and time-dependent material properties. The average drift rate was 2.5 mV/min (or ~2.5 nm/min), which corresponds to an error of 0.26% per minute of scan time. This relatively low magnitude error is easily compensated for in the post-processing of the scanned image.

5.4. Calibration grating measurements

Atomic force microscopes scan sample surfaces point by point. Each of the individual points are mapped to coordinates to form the final image. The output image of an AFM is composed of points without a meaningful physical unit. In order to obtain meaningful information from an AFM scan it is necessary to calibrate the AFM signal to samples with known dimensions. A calibration grating be used to calibrate the AFM as well as to determine the scanning resolution of the AFM. In this study, two AFM grating samples (677-AFM and 629-30, Ted Pella Inc.) were scanned to calibrate the AFM chip. The first calibration sample consisted of a layer of cellulose acetate with 500 nm line spacing and 100 nm grating height on a stainless steel disc. The second grating sample consisted of a layer of SiO_2 with 500 nm step height and period of 3 μm. The Z resolution were approximately 0.48 nm on the SiO_2 sample and 1.64 nm on the cellulose acetate sample. Differences in the Z-resolution are attributable to differences in the hardness of the samples. Amplitude Modulation AFM is most suitable for measuring hard samples such as SiO_2. Fig. 20 shows the scanning results obtained from scanning the two calibration samples in quick scan (fewer pixels), both scans can be finished in about 25 s. Lateral pixel resolution between 1.70 nm to 2.54 nm was achieved over a 1024 pixel by 1024 pixel scanning, physically the scanning windows is about 8 μm by 8 μm.

5.5. Cycle time

One of the most critical requirements of in-line metrology systems is throughput or cycle time between measurements. The system presented in this paper is capable of completing one scan cycle per minute. Total cycle time includes wafer alignment, stage-to-stage alignment, AFM approach, AFM scan, and AFM retraction.
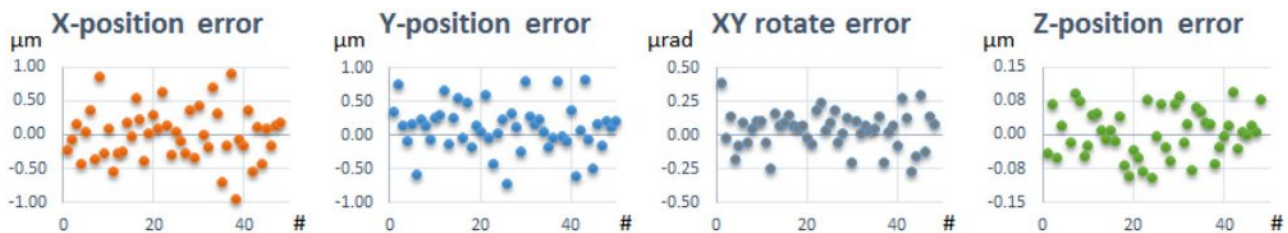

Fig. 18. Repeatability of upload/unload respectively in X, Y, and Z directions as well as in-plane rotation.

Table 2
Time budget of each step in the designed inspection system. Overall, cycle time is less than 1 min.

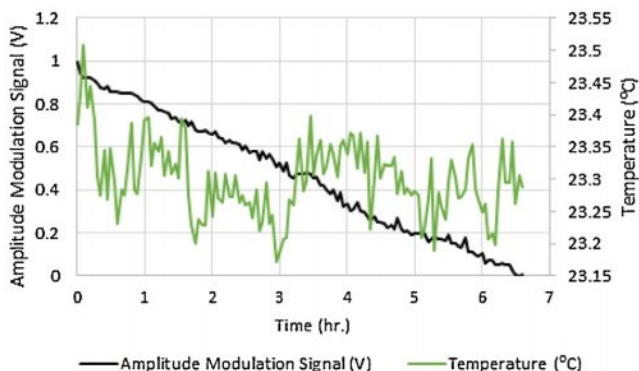|	AFM chip Exchanging	Wafer Uploading	AFM Approach	AFM Scanning	AFM Departing	Wafer Exchanging
Time Budget	0.19 s	7.07 s	5.31 s	26.05 s	0.07 s	20.55 s

Fig. 19. Time-varied cantilever signal in single-chip AFM executed in the designed inspection system as well as the ambient temperature data during execution.

The most costly step in the system is AFM scan time. Table 2 shows the time budget for each step of the inspection procedure. The major objective of this study is to minimize setup times associated with non-scanning operations such as wafer alignment, stage alignment, and AFM approach. The total setup time required for the system to be ready to scan a wafer is approximately 12 s. This is an improvement of two orders of magnitude compared to conventional AFM instruments, which require several tens of minutes to setup. Reduction in the time required to complete post-scanning operations is equally important to reduction of pre-scanning operation times. One method utilized to minimize the post-scan time is to operate the voice coil so that the AFM tip is a safe distance from the sample when no voltage is applied. This allows rapid retraction of the AFM tip from the sample by simply cutting the power supplied to the voice coil when the scan is complete. Removing the wafer sample from the setup currently takes approximately 20 s. We anticipate that it should be possible to reduce this time to less than five seconds by automating the unloading process.

One of the major issues in cycle times for traditional AFM systems is the need to periodically change out tips that have become blunted or contaminated. Realignment of the tip with the laser system and the sample can take many minutes. In the system presented in this paper, all of the sensing and actuation of the AFM tip is done directly on the AFM MEMS device. Therefore, when a chip needs to be swapped out, it is possible to just replace the entire circuit board the MEMS chip is attached to without the need to realign the chip or the sample. This enables the AMF chip replacement time to be reduced to approximately 23 s. In addition, relatively hard and blunt tips are used in this system which allows the AFMs to operate for hours before the tips need to be changed. Therefore, the total contribution of the tip changing procedure to the overall cycle time of the system is less than 1 s per cycle.

6. Discussion

The goal of this system is to enable in-line inspection for nanoscale manufacturing processes. In manufacturing processes, in-line inspection throughput must be greater than or equal to production throughput to avoid bottlenecks. The system presented is capable of inspecting one wafer every minute with the major components of time including sample removal and scanning. Advances in MEMS-based AFM systems will lead to significant reductions in
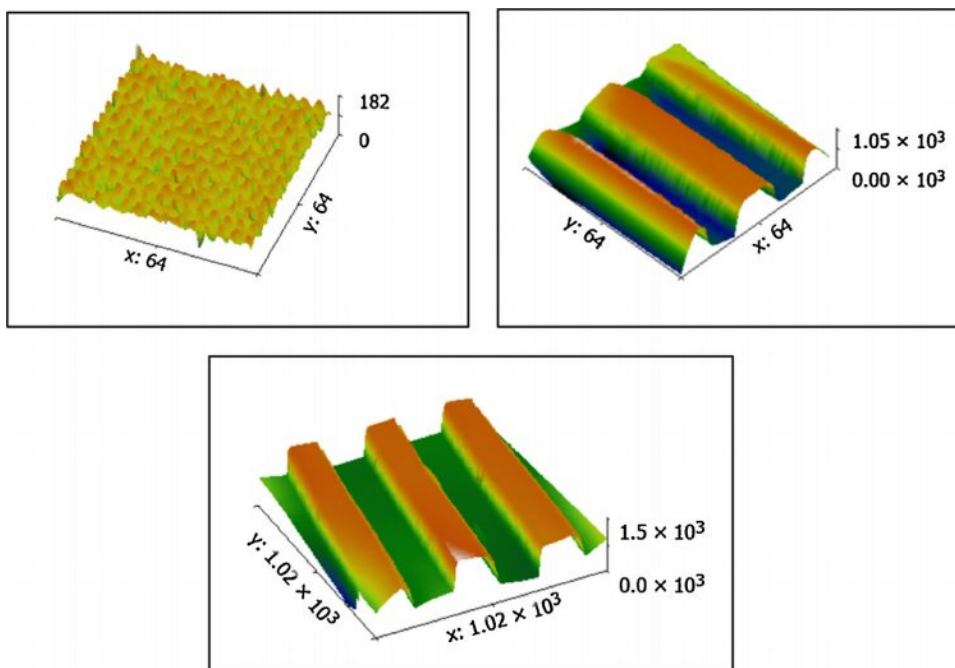

Fig. 20. AFM test imaging for grating samples which are structured with (Left) grid pattern of 500 nm line spacing and 100 nm height and (Right) 500 nm step height and period of 3 μm, 1 min of inspection procedure (Down) Higher resolution version (1024 by 1024 pixels) of 500 nm step sample.

AFM scan time. The AFM system utilized in this study was limited in speed by the bandwidth for communications between the AFM and controller. An improved interface between the AFM and its controller should lead to large reductions in scan time. Automation of the wafer removal and stage-to-stage alignment procedures could also produce time savings for non-scanning operations. Overall, these types of system improvements could help to further reduce the cycle time of the AFM system reported in this paper.

The system in this study utilizes one single-chip AFM for inspection. Due to the manual actuation of the X-Y stage attached to the flexure stage carrying the AFM chip, this stage is only capable of achieving lateral displacement resolutions of ~1 μm. In future designs of this system, the micrometer heads used in the XY positioning system can be replaced by voice coil actuators to achieve automatic control and nanoresolution motion as is currently demonstrated for the Z-axis in the propotype inspection system presented in this paper. Also, it should be possible to incorporate multiple individually actuated AFM chips into a single stage. Multiple AFM chips could be used to simultaneously inspect multiple points on a sample. Five AFM chips could be used to scan a 100-mm wafer in order to provide a large enough scan area to accurately represent the overall feature population on the wafer. The number of inspection locations on a wafer depends on the area of the wafer. Generally, semiconductor manufacturers utilize 300-mm wafers instead of the 100-mm wafers used in this study, and 450-mm wafers are expected to be in place no later than next decade. A larger sample area would allow more AFM chips to be incorporated into one stage and it is expected that a multiple AFM chip stage would scale with wafer diameter.

7. Conclusions

A system for rapid inspection of nanoscale features is presented. The system consists of a single-chip AFM, flexure-based positioning stage, and passive wafer alignment stage. The positioning stage has been examined for positioning repeatability and XY parallelism. This study uses manually operated micrometers for the XY coarse positioning. However, these micrometers can be replaced with voice coil actuators to achieve nanometer level XY course positioning resolutions in this system. Positioning resolution of the stage in Z-direction is on the order of tens of nanometers with sub-micron positioning repeatability. The AFM cantilever position exhibits low drift over short scans and the single-chip AFM is capable of scanning a 15 μm × 15 μm area with vertical resolution of 0.48 nm. The majority of cycle time is taken up by approaching the sample and new methods are being developed to minimize the time required for this step. The overall wafer in to wafer out cycle time of the system is less than 1 min. Miniaturization of moving parts has enabled high throughput scanning with single-chip AFMs and could potentially enable real-time imaging. Multiple AFM chips on a single flexure stage would allow high throughput imaging over a large area. Together, these advancements will enable true in-line metrology in semiconductor manufacturing.

Acknowledgment

References

[1] Chattopadhyay S, Huang YF, Jen YJ, Ganguly A, Chen KH, Chen LC. Anti-reflecting and photonic nanostructures. Mater Sci Eng R Rep 2010;3(June (1–3)):1–35.

[2] Leem JW, Yu JS, Heo J, Park WK, Park JH, Cho WJ, et al. Nanostructured encapsulation coverglasses with wide-angle broadband antireflection and self-cleaning properties for III–V multi-junction solar cell applications. Sol Energy Mater Sol Cells 2014;120(PART B):555–60.

[3] Yun J-H, Lee E, Park H-H, Kim D-W, an Anderson W, Kim J, et al. Incident light adjustable solar cell by periodic nanolens architecture. Sci Rep 2014;4(November):6879.

[4] Brown BP, Picco L, Miles MJ, Faul CFJ. Opportunities in high-speed atomic force microscopy. Small 2013;9(April (19)), n/a–n/a.

[5] Yao T-F, Duenner A, Cullinan MA. In-line, wafer-scale inspection in nano-fabrication systems. ASPE 2015 annual meeting 2015.

[6] Sarkar N, Lee G, Mansour RR. CMOS-MEMS dynamic FM atomic force microscope. Transducers & eurosensors XXVII: the 17th international conference on solid-state sensors, actuators and microsystems (TRANSDUCERS & EUROSENSORS XXVII) 2013;(June):916–9.

[7] Schitter G, Thurner PJ, Hansma PK. Design and input-shaping control of a novel scanner for high-speed atomic force microscopy. Mechatronics 2008;18:282–8.

[8] Malloy M, Litt LC. Technology review and assessment of nanoimprint lithography for semiconductor and patterned media manufacturing. J Micro Nanolithogr MEMS MOEMS 2011;10(3):032001.

[9] Bunday B, Germer T a, Vartanian V, Cordes A, Cepler A, Settens C. Gaps analysis for CD metrology beyond the 22 nm node. Proc SPIE 2013;8681. p. 86813B.

[10] Alvis R, Blackwood J, Lee S-H, Bray M. High-throughput, site-specific sample prep of ultra-thin TEM lamella for process metrology and failure analysis. 38th international symposium for testing and failure analysis 2012:391–7.

[11] M. Strauss, M. Williamson, Automated Transmission Electron Microscopy for Defect Review and Metrology of Si Devices (2013) pp. 366–370.

[12] Bruker Corporation, Dektak XTL Stylus Profiler System.

[13] Zygo, NewView ™ 7300 (2014).

[14] J. Richter, CD forecasting in resist by means of scatterometry (2010) 7545 Cd, pp. 754509–754509–6.

[15] McNeil JR. Scatterometry applied to microelectronics processing. Digest of the LEOS summer topical meetings. Electronic-enhanced optics. Optical sensing in semiconductor manufacturing. Electro-optics in space. Broadband optical networks (Cat. No. 00TH8497) 2000;2:II37–8.

[16] ASML, YieldStar T-250D (2016).

[17] Dunlap M, Adaskaveg JE. Introduction to the scanning electron microscope. Microsc Microanal 1997;52.

[18] Croft D, Shed G, Devasia S. Creep, hysteresis, and vibration compensation for piezoactuators: atomic force microscopy application. J Dyn Syst Meas Control 2001;123(1):35.

[19] Mamin HJ, Fan LS, Hoen S, Rugar D. Tip-based data storage using micromechanical cantilevers. Sens Actuators A Phys 1995;48(3):215–9.

[20] Hafizovic S, Barrettino D, Volden T, Sedivy J, Kirstein K-U, Brand O, et al. Single-chip mechatronic microsystem for surface imaging and force response studies. Proc Natl Acad Sci U S A 2004;101(49):17011–5.

[21] Disseldorp ECM, Tabak FC, Katan AJ, Hesselberth MBS, Oosterkamp TH, Frenken JWM, et al. MEMS-based high speed scanning probe microscopy. Rev Sci Instrum 2010;81(4):043702.

[22] Mansour RR, Lee G, Olfat M, Strathearn D, Sarkar N, Strathearn D, et al. A 0.25mm^{3} atomic force microscope on-a-chip. 28th IEEE international conference on micro electro mechanical systems (MEMS) 2015:732–5.

[23] Sarkar N, Mansour RR. Single-chip atomic force microscope with integrated Q-enhancement and isothermal scanning. IEEE 27th international conference on micro electro mechanical systems (MEMS) 2014:789–92.

[24] Lutwyche M, Andreoli C, Binnig G, Brugger J, Drechsler U, Häberle W, et al. 5×5 2D AFM cantilever arrays a first step towards a Terabit storage device. Sens Actuators A Phys 1999;73(March (1–2)):89–94.

[25] Favre M, Polesel-Maris J, Overstolz T, Niedermann P, Dasen S, Gruener G, et al. Parallel AFM imaging and force spectroscopy using two-dimensional probe arrays for applications in cell biology. J Mol Recognit 2011;24(3):446–52.

[26] Duenner A, Cullinan MA. Passive semiconductor wafer alignment mechanism to support in-line atomic force microscope metrology. ASPE 2015 annual meeting 2015.

[27] Awtar S, Parmar G. Design of a large range XY nanopositioning system. J Mech Robot 2013;5(May):1–13.

[28] Slocum AH. Design of three-groove kinematic couplings. Precis Eng 1992;14(April (2)):67–76.

[29] Attocube, Product Catalog 2015 & 2016.

[30] Lion Precision, Capacitive Product Catalog (2015).